

Characterizing FluidReflex Optical Transfer Function

Marta Victoria*, César Domínguez, Steve Askins, Ignacio Antón, and Gabriel Sala

Instituto de Energía Solar, ETSI Telecomunicación, Universidad Politécnica de Madrid, Ciudad Universitaria, 28040 Madrid, Spain

Received December 9, 2011; accepted May 7, 2012; published online October 22, 2012

FluidReflex is a novel concentrator concept that has been designed to achieve a low cost concentration photovoltaic (CPV) system over 1000× by using reflective optics and a fluid dielectric. In this paper, results regarding the characterization of the concentrator Optical Transfer Function (OTF) are presented. The reflectance and transmittance of the different materials that the concentrator is composed of have been measured using a spectrometer. In addition, a method using component cells (isotypes) has been used to experimentally determine which of the subcells within the multijunction (MJ) solar cell is limiting the current when it is illuminated by the concentrator. © 2012 The Japan Society of Applied Physics

1. Introduction

FluidReflex is a novel concentrator concept that is being developed at the IES-UPM.¹⁻⁴ It uses reflective optics to concentrate light avoiding the limit in concentration caused by chromatic aberration in refractive systems. The space between the mirror and the cell is filled with a fluid that enhances the concentrator optical efficiency by reducing Fresnel losses in several interfaces. In addition, since the solar cell is surrounded by a medium whose refractive index is higher than one the attainable concentration-acceptance angle product (CAP) is increased. The CAP is the main figure of merit in concentration photovoltaic (CPV) systems as higher concentration means lower cost whereas wider acceptance angle increases tolerance when assembling the module, aligning it and tracking the sun.

The heat concentrated in the solar cell is transported to the module walls by convection (natural or forced) and conduction in the fluid. Contrary to conventional CPV modules, where only the rear wall is warm and dissipates heat to the exterior, in FluidReflex both module walls become warm improving the heat exchange with the surrounding atmosphere. In addition, the electrical insulation in the module is enhanced, as there is no need of thermally connecting the solar cell with the cooling elements while electrically insulating this connection. Finally, the fluid acts as an encapsulating material protecting the cell from corrosion due to water vapor condensation, provided it can be proven to be harmless to the cell and the rest of the module components. Several fluid candidates⁵ are being investigated in order to choose the most appropriate based on both optical and thermal properties, as well as its performance under accelerated UV degradation tests. The results addressed in this paper correspond to one of the most suitable candidates: paraffin oil. A FluidReflex elementary unit consists of a paraboloid mirror, a high efficiency multijunction (MJ) solar cell placed in its focus and the dielectric fluid filling the volume between the mirror and the cell plane (Fig. 1). Square mirrors are placed in a grid to create an array of 16 × 10 elements that constitutes the module whose external dimensions are approximately 800 × 500 × 35 mm³.

As a first step in the transition from the theoretical concept to a real CPV system, several elementary unit prototypes were manufactured and characterized. By using the same

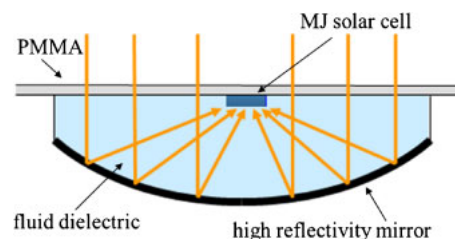


Fig. 1. (Color online) FluidReflex concentrator scheme.

paraboloid mirror and solar cells with different diameters, several systems with geometrical concentrations 1314×, 1035×, 584× were built. The measured acceptance angles were ±0.65, ±0.92, and ±1.4° respectively which is in good agreement with what it is predicted by theory and confirms the high CAP attainable by using a fluid dielectric.² Acceptance angle is defined as the deviation angle such that efficiency is 90% of its maximum and was measured indoors using a CPV solar simulator.⁶ In addition, an optical efficiency of 83.5% at 1035× has been measured for the best performing prototype.⁴ This result was obtained for a high reflectivity silver over poly(methyl methacrylate) (PMMA) mirror and using a solar cell whose antireflective coating (ARC) has been optimized for the particular light distribution created by the concentrator optics.⁷

The FluidReflex concentrator has been designed to use MJ solar cells since they are the photovoltaic devices with the highest efficiency. Triple-junction solar cells are currently a mature technology after several years of intensive research. In addition, that number of junctions seems to be a good trade-off between maximizing the cell efficiency and allowing some tolerance to spectral changes.⁸ An extensively investigated triple-junction solar cell is the lattice-matched GaInP/GaInAs/Ge grown over a Ge substrate. This combination of semiconductor materials has reached a record efficiency of 41.6%⁹ and it is commercially available at efficiencies around 40%.

Figure 2 shows the quantum efficiency (QE) of a typical MJ solar cell of this technology. Since subcells are series connected the minimum photogenerated current will limit the total cell current and consequently the cell efficiency. Under the reference direct spectrum AM1.5D¹⁰ the germanium bottom subcell photogenerates an excess of current so the cell under non-concentrated illumination is usually either top or middle limited.

*E-mail address: marta.victoria@ies-def.upm.es

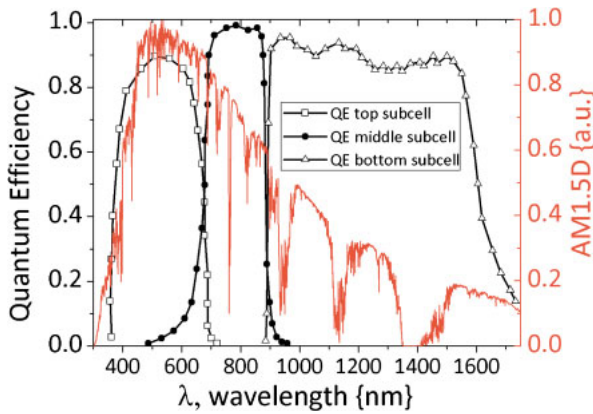


Fig. 2. (Color online) QE of a lattice-matched GaInP/GaInAs/Ge triple-junction solar cell currently commercially available. Superimposed direct spectrum AM1.5D.¹⁰⁾

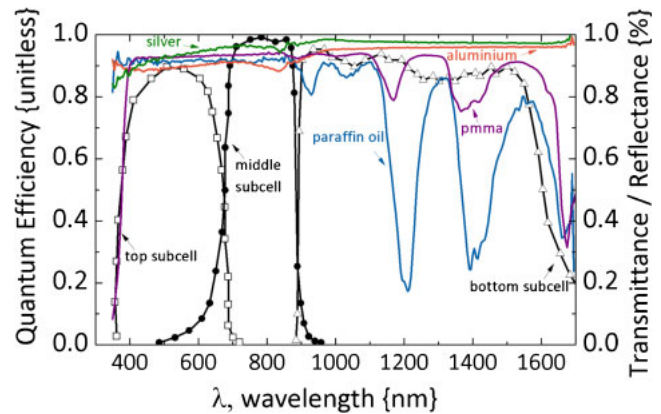


Fig. 3. (Color online) QE of a lattice-matched GaInP/GaInAs/Ge triple-junction solar cell currently commercially available. Superimposed transmittance of the fluid used in FluidReflex concentrator and reflectance of the two mirrors under study: aluminum and silver evaporated mirrors.

A new triple-junction solar cell architecture consisting of using an epi-growth process with GaAs substrate has shown very promising results obtaining an efficiency of 42.5% for a GaInP/GaAs/GaInAs solar cell¹¹⁾ and 43.5% for the GaInP/GaAs/GaInNAs configuration.¹²⁾ However, it still remains to be proven if the efficiency enhancement makes up the increase in the manufacturing process complexity, the associated reliability uncertainties and the spectral sensitivity increment.

Due to the fact that MJ solar cells are sensitive to a very wide wavelengths range (350–1800 nm) and tacking into account that they are series connected, it is extremely important to characterize the optical transfer function (OTF) of any concentration system to be used. The methods described in this paper are focus on characterizing FluidReflex concentrator OTF. However, these methods could also be applied similarly to characterize any other CPV system.

2. Experimental Procedure

The first experimental method applied to characterize concentrator OTF consists in the use of a spectrometer to measure the spectral behavior of every material to be used, including the reflectance of aluminum and silver mirrors (Fig. 3). Special emphasis was placed on measuring transmittance of dielectric-fluid candidates⁵⁾ as they have never been used in photovoltaics before. A visible–near-infrared spectrophotometer (Instruments Systems VIS-NIR1 SPECTRO 320) was used to perform the measurements. Transmittance and reflectance were measured from 350–1700 nm for a 5 nm interval. For the reflectance measurements, samples were manufactured evaporating silver and aluminum over flat PMMA substrates. The fluid was contained in a quartz cuvette with negligible absorbance in all the wavelengths measured. A flat 2-mm-thick sample was used to measure PMMA transmittance. To clarify the nomenclature, the transmitted light is the remainder when the reflected and absorbed portions are subtracted from the incident flux.

The second applied method was already presented in ref. 14 and it allows the direct experimental determination of the limiting subcell within a MJ solar cell illuminated by a

concentrator. In this method, the concentrator is irradiated by a collimated light beam at 850 W/m² created by a flash solar simulator specifically designed for measuring CPV systems.⁶⁾ To monitor the spectral distribution of light emitted by the flash lamp, the short-circuit currents of three “isotype” cells (top, middle, and bottom) inside collimating tubes are recorded for each measurement. An “isotype” is equivalent to a MJ solar cell in which only one of the subcells is electrically connected. Hence, they behave optically as a MJ solar cell but the photogenerated current corresponds to the connected subcell independently of the spectral distribution of the incident light.

Thus, using the information provided by the “isotypes”, a figure of merit can be defined to describe the spectrum of the flash light: the spectral matching ratio (SMR) [eq. (1)]. It is defined as the ratio between top and middle subcell photogenerated currents under the spectrum in study, divided by that ratio under the reference spectrum. SMR can be calculated as

$$\text{SMR (AM1.5D)} = \frac{I_{L,\text{top}}(E_{\text{simulator}})/I_{L,\text{middle}}(E_{\text{simulator}})}{I_{L,\text{top}}(\text{AM1.5D})/I_{L,\text{middle}}(\text{AM1.5D})}, \quad (1)$$

where $I_{L,i}(E_{\text{simulator}})$ represents the photocurrent of a subcell (top or middle) when illuminated with a particular spectral irradiance distribution $E_{\text{simulator}}$ under the simulator and $I_{L,i}(\text{AM1.5D})$ stands for the photoresponse of a subcell under the reference spectrum. SMR is an indicator of how blue-shifted ($\text{SMR} > 1$) or red-shifted ($\text{SMR} < 1$) the light is with respect to the reference spectrum. An important point about the experimental method used is that the SMR and the irradiance are varied simultaneously, because of intrinsic properties of the light source: the spectrum shifts from blue to red during the flash pulse decay.

During this flash decay, the currents generated by the MJ solar cell inside the FluidReflex concentrator (device under test, DUT) and the three isotypes solar cells (top, middle, and bottom) are recorded simultaneously. Normalized currents are calculated using this data [eq. (2)]. A normalized current $I_{N,\text{subcell},i}$, is defined as the ratio between the DUT current $I_{L,\text{DUT}}$, and the irradiation level experienced by the correspondent “isotype” i which in turn can be calculated as the ratio between the “isotype” current under

the simulator spectrum $I_{L,subcell_i}(E_{simulator})$, and its photo-response under the reference spectrum $I_{L,subcell_i}(AM1.5D)$:

$$I_{N,subcell_i} = \frac{I_{L,DUT}}{I_{L,subcell_i}(E_{simulator})/I_{L,subcell_i}(AM1.5D)}. \quad (2)$$

Once normalized currents have been calculated for the three subcells if they are plotted as a function of SMR the limiting subcell is graphically exposed in a very clear manner. When the normalized current for a given subcell remains constant during a certain portion of the flash decay, that is the limiting subcell for the corresponding spectral range (the evolution of current with irradiance in the DUT is proportional to the evolution of that particular subcell current). Conversely, the normalized current for non-limiting (saturated) subcells will be constantly changing as the spectrum changes.

3. Results and Discussion

Figure 3 shows the measured transmittance and reflectance for the materials that are part of FluidReflex concentrator system. Reflectance has been measured for two candidate mirrors: aluminum and silver, in both cases evaporated over PMMA. Silver reflectivity is higher than aluminum for all the wavelengths range MJ solar cells are sensitive to except for wavelengths lower than 350 nm. Hence, light useful for the top subcell will be reduced in case of using silver although it doesn't seem very critical. Silver mirrors are not commonly used in CPV systems due to the usual degradation caused by outdoor exposure. However, for this particular concentrator dielectric fluid may protect silver avoiding its corrosion. At the moment degradation experiments are ongoing and both materials are considered suitable candidates. Reflectance was measured, in both cases, for first surface mirrors; hence they represent the reflectance of aluminum and silver when those materials are surrounded by air. It must be taken into account that in real FluidReflex concentrator the mirror will be immersed in a fluid whose refractive index is higher than one and consequently a slightly lower reflectivity will be obtained¹⁴⁾ (in detail calculation of this effect can be found in ref. 5).

Regarding the dielectric fluid transmittance, Fig. 3 shows the measured values for a 40 mm sample of paraffin oil. The sample length was chosen to be equal to the optical path of the light within the concentrator. Three important transmittance valleys appear at 900, 1150, and 1350 nm, all of them are in the bottom subcell region. Because those valleys are due to carbons bonds of the molecules the fluid is composed of they also appear when measuring plastics transmittance.^{15,16)} Consequently if the module walls are made of PMMA, low transmittance regions for the fluid will be coincident to those in the plastic and the total absorbance losses will not increase significantly.

The OTF of the system can be estimated as the product of transmittance at the entrance of the system $[1 - R_{entrance}(\lambda)]$, the front wall plastic transmittance $T_{plastic}(\lambda)$, the mirror reflectance $R_{mirror}(\lambda)$, and the fluid transmittance $T_{fluid}(\lambda)$. The photogenerated current density of each subcell $J_{subcell_i}$, can be calculated by integrating its spectral response $SR_{subcell_i}(\lambda)$, multiplied by the reference spectrum $B_{AM1.5D}(\lambda)$, and the $OTF(\lambda)$ of the system. The total cell photogenerated current density J_{cell} , will be the minimum of the three $J_{subcell_i}$:

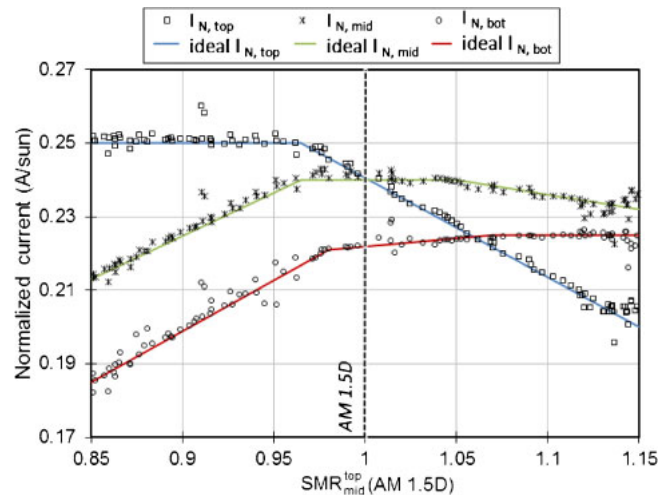


Fig. 4. (Color online) Evolution of the ratio between photogenerated current of MJ solar cell illuminated by the concentrator and irradiance “seen” by each “isotype” solar cell (normalized current) as a function of SMR. Horizontal data points out the limiting subcell for each spectral distribution of the incident light quantified by SMR.

$$\begin{aligned} J_{cell} &= \min J_{subcell_i} \\ &= \min_{subcell_i} \left[\int_{\lambda_{max}}^{\lambda_{min}} SR_{subcell_i}(\lambda) B_{AM1.5D}(\lambda) OTF(\lambda) \partial\lambda \right] \\ &= \min_{subcell_i} \left[\int_{\lambda_{max}}^{\lambda_{min}} SR_{subcell_i}(\lambda) B_{AM1.5D}(\lambda) \right. \\ &\quad \left. \times [1 - R_{entrance}(\lambda)] T_{plastic}(\lambda) R_{mirror}(\lambda) T_{fluid}(\lambda) \partial\lambda \right]. \quad (3) \end{aligned}$$

The currents photogenerated by each subcell when being illuminated by the concentrator can be estimated by multiplying the current density J_{cell} by the cell area A_{cell} , and the geometrical concentration X_{geo} :

$$J_{subcell_i} = A_{cell} X_{geo} J_{subcell_i}. \quad (4)$$

As an example, for the FluidReflex prototype comprising a 2.3 mm diameter solar cell and a square silver-over-PMMA mirror at 584×, calculated photogenerated currents for top, middle, and bottom subcells are respectively 0.248, 0.243, and 0.258 A.

The results of the second method, which allows the direct experimental determination of the limiting subcell, can be observed in Fig. 4. As was previously explained, when the normalized current remains constant for one of the subcell it indicates that this is the limiting subcell. Evolution on the light spectral content as the pulse decays can be read in Fig. 4 from right to left (as the irradiance intensity decreases spectrum becomes redder and SMR decreases). Figure 4 clearly shows that at the beginning of the pulse decay, when the spectrum is blue-shifted ($SMR > 1$), the current is limited by the bottom subcell. At $SMR = 1.05$ middle subcell starts to limit the current and the same limitation mode is maintained for the situation equivalent to the reference spectrum AM1.5D ($SMR = 1$) and until $SMR = 0.97$. This result is in agreement to the first method which predicted a middle limitation under the reference spectrum. The bottom subcell shows the greatest difference between estimated and measured photocurrent. Experimental errors

when measuring transmittance and reflectance is a plausible explanation for this disagreement.

In conclusion, the second proposed experimental method has resulted very useful in directly determine the limiting subcell inside a concentrator under variable spectral distribution of the incident light. The method has proven to be useful not only to characterize the concentrator performance under reference spectrum but also to analyze its spectral sensitivity which is crucial to estimate its outdoor performance under variable spectral conditions.

Acknowledgements

This work has been partially supported by European commission within the project NACIR (226409-2) under the VII Framework Program. M. Victoria work is directly supported by Spanish Ministry of Science and Innovation under an FPI grant.

-
- 1) M. Victoria, C. Domínguez, I. Antón, and G. Sala: Proc. 23rd European Photovoltaic Solar Energy Conf., 2008, p. 132.
 - 2) M. Victoria, C. Domínguez, S. Askins, I. Antón, and G. Sala: Proc. 6th Conf. Concentration Photovoltaics, 2010, p. 118.
 - 3) M. Victoria, E. Chiappori, S. Askins, C. Domínguez, I. Antón, and G. Sala:

- Proc. 25th European Photovoltaic Solar Energy Conf., 2010, p. 902.
- 4) M. Victoria, S. Askins, C. Domínguez, I. Antón, and G. Sala: Proc. 7th Conf. Concentration Photovoltaics, 2011, p. 253.
- 5) M. Victoria, S. Askins, C. Domínguez, I. Antón, and G. Sala: submitted to Prog. Photovoltaics.
- 6) C. Domínguez, I. Antón, and G. Sala: *Opt. Express* **16** (2008) 14894.
- 7) M. Victoria, C. Domínguez, I. Antón, and G. Sala: *Opt. Express* **20** (2012) 8136.
- 8) K. Araki, M. Kondo, H. Uozumi, and M. Yamaguchi: Proc. 3rd World Conf. Photovoltaic Energy Conversion, 2003.
- 9) R. R. King, A. Boca, W. Hong, X.-Q. Liu, D. Bhusari, D. Larrabee, K. M. Edmondson, D. C. Law, C. M. Fetzer, S. Mesropian, and N. H. Karamet: Proc. 24th European Photovoltaic Solar Energy Conf., 2009, p. 55.
- 10) Reference direct spectrum ASTM G173-03 derived from SMARTS.
- 11) S. Wojtczuk, P. Chiu, X. Zhang, D. Derkacs, C. Harris, D. Pulver, and M. Timmons: Proc. 35th IEEE Photovoltaic Specialist Conf., 2010, p. 1259.
- 12) M. A. Green, K. Emery, Y. Hishikawa, W. Warta, and E. Dunlop: *Prog. Photovoltaics* **19** (2011) 565.
- 13) C. Domínguez, I. Antón, G. Sala, and S. Askins: Prog. Photovoltaics (in press) [DOI: [10.1002/pip.2227](https://doi.org/10.1002/pip.2227)].
- 14) M. Born and E. Wolf: *Principles of Optics* (Pergamon Press, Oxford, U.K., 1959) 6th ed.
- 15) J. D. Lytle: in *Handbook of Optics*, ed. M. Blass (McGraw-Hill, New York, 1995) Vol. II, Chap. 34, p. 1171.
- 16) O. Ziemann, J. Krauser, P. E. Zamzow, and W. Daum: *POF Handbook* (Springer, Berlin, 2008).
- 17) A. Luque, J. M. Gómez, A. Cuevas, J. Eguren, and E. Lorenzo: Solar Energy Symp., 1978.
- 18) T. Ugumori and M. Ikeya: Proc. 2nd Photovoltaic Science and Engineering Conf. Japan, Tokyo, 1980, Jpn. J. Appl. Phys. **20** (1981) Suppl. 20-2, p. 77.